Sigma Journal of Engineering and Natural Sciences
Web page info: https://sigma.yildiz.edu.tr
DOI: 10.14744/sigma.2022.00011

Research Article

Green synthesis of BT-Fe_3O_4 nanocomposite using *Camellia sinensis* leaves extract: Characterization, NPEO adsorption experiments, isotherms, and kinetics

Pınar BELİBAĞLI[1], Yağmur UYSAL[1,*]

[1]*Mersin University, Department of Environmental Engineering, Mersin, Turkey*

ARTICLE INFO

Article history
Received: 22 January 2021
Accepted: 15 March 2021

Key words:
Adsorption; Black-tea; green synthesis; Magnetite nanocomposite; Nonylphenol ethoxylate

ABSTRACT

In this study, Black Tea-Fe_3O_4 (BT-Fe_3O_4) magnetite nanocomposites was synthesized from extract of black tea (BT-*Camellia sinensis*) leaves with an eco-friendly method, and used to investigate nonylphenol ethoxylate (NPEO) removal potential from water. The results of the characterization determination studies performed on the adsorbent revealed that the herbal extract obtained from black tea leaves successfully covered the surface of magnetite (Fe_3O_4) nanoparticles. Batch tests were carried out to define the action of BT-Fe_3O_4 dose, initial NPEO concentration, pH and contact time on the adsorption attitude of the BT-Fe_3O_4. Adsorption isotherms and kinetics were described by a Freundlich isotherm model and pseudo-second-order kinetic model. The experimental results showed that maximum adsorption efficiency of NPEO (%73.45) occurred the optimal pH value of 7.0, NPEO concentration of 10 mg/L, BT-Fe_3O_4 dose of 1g/L, and contact time of 60 minutes. The results of the study have shown that BT-Fe_3O_4 particles have promising applicability in the removal of NPEO from aqueous media by adsorption method as an environmentally friendly and low-cost alternative adsorbent with rapid separation ability for wastewater treatment.

Cite this article as: Belibagli P, Uysal Y. Green synthesis of BT-Fe_3O_4 nanocomposite using *Camellia sinensis* leaves extract: characterization, npeo adsorption experiments, isotherms, and kinetics. Sigma J Eng Nat Sci 2022;40(1):133–144.

INTRODUCTION

According to results of the research conducted by the World Wide Fund for Nature (WWF) and Eurostat, worldwide chemical production has been increasing exponentially since 1903. In 2017, 97.8 million tons of these chemicals were reported to be harmful to the environment and health [1]. Nonylphenol ethoxylates (NPEO) are

***Corresponding author.**
*E-mail address: yagmuruysal@gmail.com

This paper was recommended for publication in revised form by Regional Editor Nergis Arsu

produced approx. 400,000 tons of year worldwide. NPEOs are one of the commonly used nonionic surfactants, and consist of a hydrophobic structure with a hydroxyl group, a phenol ring and a linear nonyl chain in the para position [2]. The increasing industrial demand for NPEOs and their usage in anthropogenic activities have increased their emergence as a contaminant in drainage mud and garbage dump sites due to waste evacuation, water treatment plants, and random dumping [3, 4].

NPEO has been detected in streams at concentration switching from 2.5 to 97.6 μg/L [5] and risk coefficient greater than 1.0 indicating that may pose significant ecotoxicological risks [6]. Nonylphenol (NP) in the medium originates from the degradation of nonylphenol ethoxylates (NPEOs) [7]. According to previous studies, the average NP concentration in sewage sludge used for soil improvement was determined as 24.907 mg/kg [8]. It has been determined that NP concentration in wastewater treatment plants is measured as 0.79 μg/L and this value can reach up to 0.1-1.2 mg/L around contaminated rivers and septic systems [9]. Various studies have shown that NPs can mimic natural estrogens withal the estrogen receiver, thus inhibiting the activity of the hormone, bioaccumulating in aquatic organisms, altering the endogenous levels of steroids, diabetes, reproductive system, and is associated with obesity [4, 10-13]. Consequently, numerous countries have restricted the use of NPEO surface-active agents [14]. The current policy on NP in the European Commission is to ban its use within the European Union through the 2003/53/EC Directive. [15].

Many technologies such as biological, physical, and biotechnological methods have been applied to separate or treat NPEOs from wastewater. Combined methods for adsorption and enhanced oxidation processes (ie. photocatalysis) are attractive as they get the benefit of synergistic impacts [2, 16]. It has been viewed that adsorption is one of the very effective, economic, and effortless methods for contaminant removal. However, the transmission of complexes into the solid phase owing to adsorption can beget a seconder contaminant in water. This issue could be intercepted by adopting an alternative way such as nanomaterials based photo-catalysis [17-19]. Nevertheless, there are few studies on the synthesis of nanomaterials that meet all these criteria. Therefore, green synthesis methods that are environmentally, economically, and technically feasible are needed instead of traditional methods [20]. Nanomaterials produced using herbal phytochemicals notably decrease environmental contaminants, aid economically viable and sustainable neat and green chemistry technologies [21].

The selection of green synthesis routes may conduct significant benefits over the traditional process. For example, traditional processes tend to produce waste (liquid or solid), which often signals the use of costly chemicals and additional investments in the treatment of these pollutants [22-25]. Plant-based nanomaterial synthesis is preferred as it can be produced from a large number of different natural substances, and powerful biomolecular reducing agents can be obtained from a variety of plants [26]. It has been reported that plants contain a wide variety of antioxidants and secondary metabolites, and these biomolecules work in harmony to inhibit cellular components [27, 28]. Plant extracts contain reducing and stabilizing agents for the synthesis of magnetite nanoparticles such as phenols, carboxylic acid, and amino acids [29, 30]. Black teas within the *Camellia sinensis* family grow in temperate and tropical areas. The rich source of polyphenols in the structure of black tea leaves acts as a reducing agent in the synthesis of metal nanoparticles [31].

The fundamental goal of this paper is to investigate the potential of green synthesized BT-Fe_3O_4 composite to adsorb environmentally harmful nonylphenol ethoxylates as adsorbent material. The novelty of this study is to obtain a new magnetite composite material using Black Tea leaves (an eco-friendly stabilizing matter for the synthesis of magnetite materials) so combine these properties in a single substance. Also to our knowledge, preparation, and application of BT-Fe_3O_4 for NPEO removal in solutions have not yet been studied. Experimental studies were conducted as follows: (1) Characterization of green synthesized BT-Fe_3O_4 to control the chemical species on the surface of the nanomaterial and the changes in its structure before and after NP adsorption; (2) Batch adsorption experiments performed to optimize various parameters such as pH, nano-dose, initial NPEO concentration and contact time; and (3) Kinetic studies to examine the stability of the adsorption isotherm and the adsorption process.

MATERIAL AND METHODS

MATERIALS

NPEO stock solution (1000 mg/L) was prepared from nonylphenol ethoxylate (Acar Chemistry). All chemicals such as NH_4OH, $FeCl_3.6H_2O$, $FeCl_2.4H_2O$, HCI and NaOH (Merck) used in the synthesis of magnetite nano-composites and required for experiments were analytical reagents.

Green Synthesis of Magnetite Nanomaterials From Black Tea (Camellia Sinensis) Extract

First, the purchased black tea leaves were washed several times with distilled water, to remove dust and dirty and dried. Then tea extract was prepared by boiling 30g/0.5L of the leaves of that plant at 80°C for 1h. After precipitation for 1 h, the extract was filtered. Then a magnetite nanopar-ticle (Fe_3O_4) solution was prepared by adding 6.1278 g of solid $FeCl_3.4H_2O$ and 3.0121 g of solid $FeCl_2.6H_2O$ into 100 mL of deionized water under N_2 medium. When the solution temperature reached to 85°C, 25 mL of 25% purity ammonia (NH_3) solution was stirred for 2 min. to

be a homogeneous mixture. Then tea extract was added and the reaction was stirring out in nitrogen for during 30 min and cooled to room temperature. At this time, a black precipitate formed, evidencing the formation of BT-Fe_3O_4 particles. The BT-Fe_3O_4 nanoparticles formed were washed several times with distilled water and separated with neodymium magnet [32, 33].

Instrumental Analyzes

High-performance liquid chromatography (HPLC-Shimadzu LC-20AD) equipped with a fluorescence detector was used for measuring of NPEO concentrations. The morphology and size of the resulted BT-Fe_3O_4 particles were characterized by Field Emission Scanning Electron Microscopy (FE-SEM). Fourier Transformed Infrared Spectroscopy (FT-IR) was realized by FT-IR-410.

Batch Studies

Batch studies were performed in an orbital shaker with a constant speed of 200 rpm in 100mL flasks. After that, NPEO solutions were centrifuged (4000 rpm), and the solutions of NPEO in the supernatant solutions were analyzed by using an HPLC. The main process parameters considered were pH (3.0, 5.0, 7.0, 9.0, 11.0), initial NPEO concentration (10, 20, 40, 60, 80 mg/L), nanoparticle dose (1, 2, 4, 6, 8 g/L), and contact time (10, 20, 40, 60, 90 min). For the accuracy of the results obtained, the experiments were repeated twice and their average result reported.

The removal percentage (%) of NPEO was calculated for as follows each run by using Equation (1)

$$\%\ \text{removal} = \frac{C_0 - Ce}{Ce} \times 100 \quad (1)$$

where C_0 (mg/L) and Ce (mg/L) are the initial and balance concentrations of NPEO.

RESULTS AND DISCUSSION STRUCTURE ANALYSIS OF BT-FE_3O_4

SEM surface analyses of the BT-Fe_3O_4 particles before and after the adsorption were used to identify synthesized particles, and were shown in Fig. 1(a-b). Before the adsorption process, nanocomposite particles had an irregular and rough surface (Fig 1a). In Figure 1b, it was observed that after adsorption of NPEO removal, the nanoparticles generally exhibited rough surface morphology and flocculation was dominant.

The FTIR spectrum of the nanoparticles produced was also shown in Fig. 2. For raw Fe_3O_4 spectrum, the peaks at 1593.15 cm^{-1} and 549.93 cm^{-1} belonged to the C=C stretching and Fe stretching vibrations, respectively [34]. Before the adsorption process, for BT-Fe_3O_4, the peaks at 3126.37-2989.71 cm^{-1} correspond to the stretching vibration of C-H (aliphatic) bending. The peaks at 1605.50 and 1401.63 cm^{-1} show C=C (aromatic), and C-N bonds, respectively. The peak at 1060.15 cm^{-1} corresponds to C-O bonds. As shown in Fig. 2, the adsorption peaks at 549.93 cm^{-1}, 1060.15 cm^{-1} and 1401.63 cm^{-1} were related with the Fe_3O_4 nanoparticles coated with black tea. After the adsorption process, the peak at 3369.84 cm-1 for BT-Fe_3O_4 related to the tension vibration of O-H.

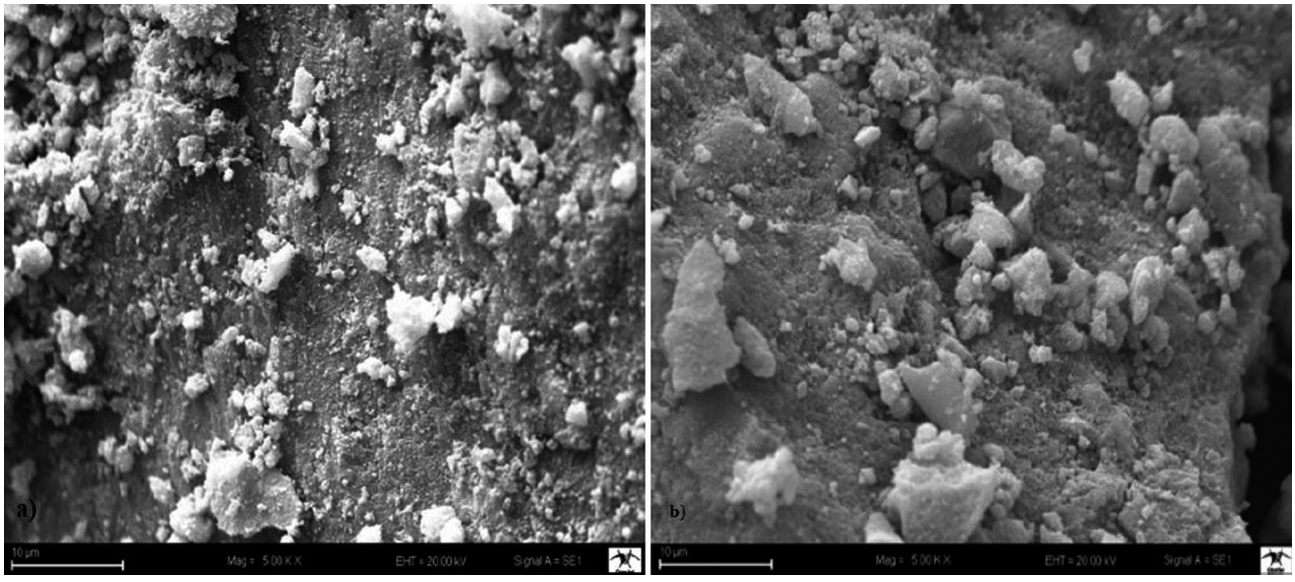

Figure 1. SEM analyses of BT-Fe_3O_4 before (a) and after adsorption (b) with adsorbed NPEO.

Sigma J Eng Nat Sci, Vol. 40, No. 1, pp. 132-143, March, 2022

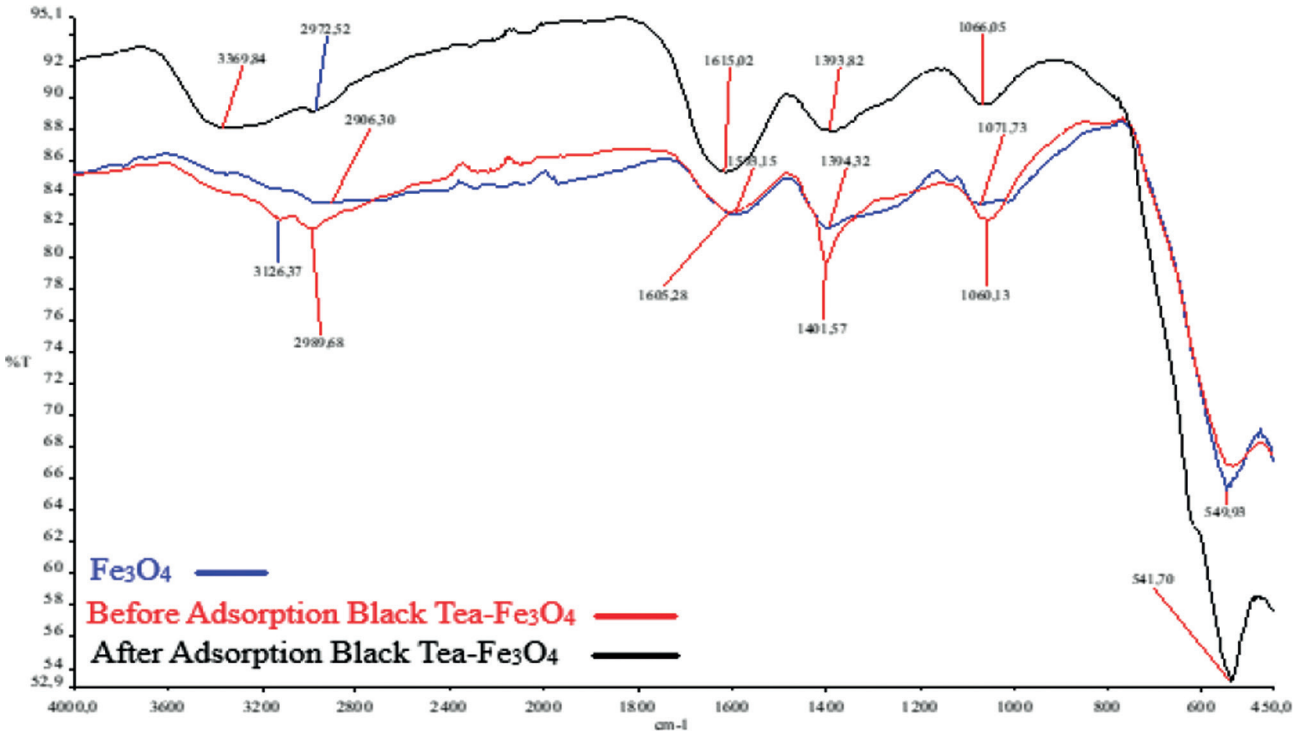

Figure 2. FT-IR spectrum of adsorption of BT-Fe_3O_4.

ADSORPTION STUDIES

Effect of PH on the Process

The effect of different pH values (3.0-11.0 range) on the adsorption processes was given in Fig. 3. According to experimental studies to determine the pH effect on the adsorption process up to 90 min, it was determined that NPEO removal efficiency decreased with increasing after pH 7.0. This reduction is not a high reduction. The adsorbent has a high removal efficiency potential in the pH range of 3.0-7.0. There was only a slight decrease in removal efficiency at pH 9.0 and above. The maximum NPEO removal efficiency was obtained at pH 4.0 as 74%. Maximum adsorption yield at low pHs can be described as the interplay between the dipole of phenol function in NPEO and the positively charged BT-Fe_3O_4 surfaces [37]. In addition, low pH which is full of hydrogen ions in NPEO solution, and the effect of the propelling force of dense aromatic bonds (π-π) have led to an increase in hydrogen bond adsorption efficiency [38]. However, in alkaline conditions, the surface of BT-Fe_3O_4 particles is negatively charged and repulsion takes place between Bt-Fe_3O_4 and NPEO molecules, and the adsorption efficiency decreases [39]. When the obtained pH results were evaluated, as the adsorbent structure could degrade at low pH [40] and the removal efficiency was almost the same between pH 3.0 and pH 7.0, 7.0 was chosen as the optimum pH for NPEO removal and the experiments continued at pH.

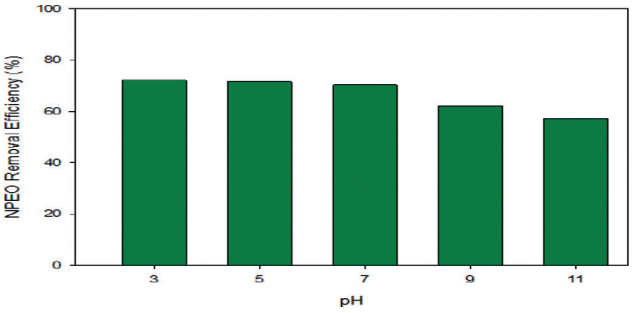

Figure 3. pH on NPEO treatment.
(BT-Fe_3O_4: 4g/L, NPEO Concentration: 20 mg/L, T: 25°C)

Effect of BT-FE_3O_4 Dose on the Process

The effect of BT-Fe_3O_4 nano-dose on the NPEO removal adsorption process was shown in Fig.4. Increasing of BT-Fe_3O_4 nano-dose showed that there was no significant change in the removal efficiency, and NFE removal was independent of the nanocomposite dose. The fact that the removal efficiency does not change at high adsorbent concentrations reveals that there will be no need for high adsorbents and that the desired treatment efficiency can be achieved with a low amount of adsorbent. Thus, optimum nano-dose 1 g/L was selected for NPEO removal (72.25%) and the experiments continued with this dose.

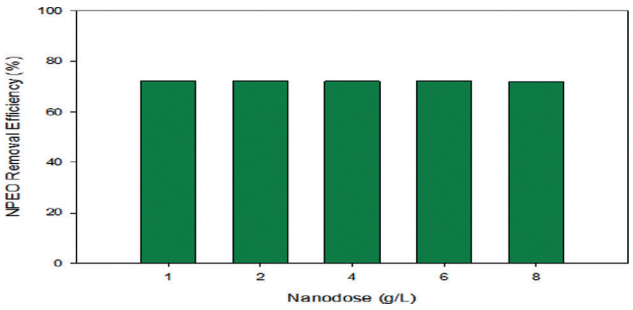

Figure 4. BT-Fe_3O_4 on NPEO treatment.
(pH: 7.0, NPEO Concentration: 20 mg/L, T: 25°C)

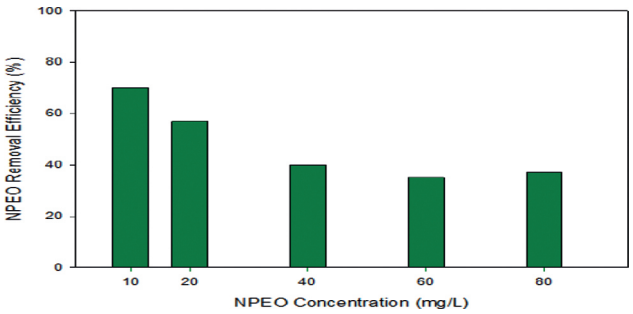

Figure 5. NPEO concentration on NPEO treatment.
(pH: 7.0, BT-Fe_3O_4 quantity: 1g/L, T: 25°C)

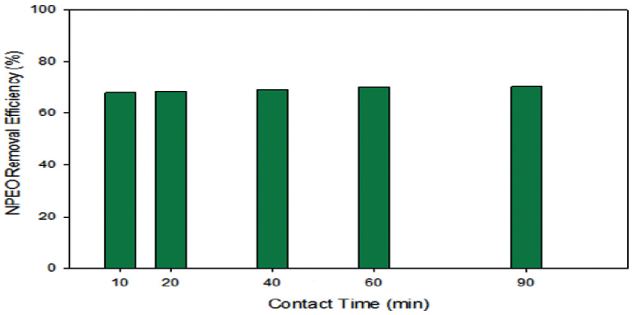

Figure 6. Contact time on NPEO treatment.
(pH: 7.0, BT-Fe_3O_4 quantity: 1g/L, NPEO Concentration: 10 mg/L, T: 25°C)

Effect of NPEO Concentrations on the Process

The effect of initial NPEO concentrations on the treat-ment process of NPEO was shown in Fig.5. Figure 5 showed that the increasing of NPEO concentrations induce a nota-ble reduction in the treatment efficiency of BT-Fe_3O_4. This behavior is due to the filling of functional groups on the BT-Fe_3O_4 surface due to the increase in the initial NPEO concentrations of BT-Fe_3O_4 particles [41]. While removal efficiency was achieved at 70% values at 10 mg/L NPEO concentration, removal efficiency continued at 40% at con-centrations where the NPEO concentration in the envi-ronment increased to 40 mg/L and above. This shows that this adsorbent can be used efficiently for wastewater with NPEO concentrations of 10 mg/L or less, depending on the desired treatment efficiency.

Effect of Time on the Process

The impact of time on the removal efficiency of NPEO by BT-Fe_3O_4 was investigated at various reaction times (10–90 min). Figure 6 shows that removal efficiency does not change significantly with time. A removal efficiency in the range of 60–70% has been achieved in the first 10 minutes from the start of the adsorption. This yield increased slightly up to 60 minutes, and did not change significantly when the time was extended to 90 minutes. This revealed that the adsorbent reached saturation in a very short time. The retention time reaching equilibrium in 60 minutes can be explained by filling all active sites of BT-Fe_3O_4 particles with NPEO [42].

The adsorption capacity of BT-Fe_3O_4 for NPEO species was compared with adsorbents previously reported (Table 1). In general, the BT-Fe_3O_4 nanocomposites have exhibiting faster equilibrium time and nearly the same adsorption efficiency than almost all listed adsorbents. At the same time, the presence of the black tea structure together with the magnetic properties of the adsorbent reveals that an environmentally friendly, low-cost BT-Fe_3O_4 adsorbent with fast separation capability can be used as a promising solution for NPEO adsorption.

ISOTHERM MODELS

Isotherms studies are a useful tool to forecast the adsorbent effectiveness to removal a given pollutant from polluted water/wastewater. In order to define the model of NPEO removal on the BT-Fe_3O_4, isotherms were determined by exposing various doses of the adsorbent. The other affecting factors were kept constant. The parameters and correlation coefficients (R^2) were summarized in Table 2 and Figure 7 (a, b, c, d). According to the fixed parameters shown in Table 1, the values of n and R_L less than 1.0 showed that NPEO adsorption was positive. The results showed that the degree of fit for the Freundlich model was higher than that for the Harkins-Jura model.

KINETIC MODELS

Kinetic studies are significant for the estimate of optimum conditions in the full-scale adsorption processes [49]. Three different kinetic models were used to determine the time-dependent variation of NPEO adsorption on BT-Fe_3O_4 and its adsorption rate. In order to study the mechanism of

Sigma J Eng Nat Sci, Vol. 40, No. 1, pp. 132-143, March, 2022

Table 1. Comparison of the maximum efficiency and adsorption capacities of NPEO on various adsorbents

Adsorbent	Optimal conditions	Adsorption capacity or removal efficiency	Ref.
PAMAM-MNP (polyamidoamine magnetite nanoparticles)	NPEO: - pH: 7.0 Contact Time: 60 min Temp.: 30°C	Distilled water: 70% Drinking water: 67% Well water: 63% Treated wastewater: 65%	[43]
Fe_3O_4/AC (magnetite-activated carbon)	NPEO: 1–5 mg/L pH: 3.0 Contact Time: 30 min Temp. 25°C	73.3%	[44]
Fly-ash-cenospheres/Fe_3O_4	NP: 2mg/L pH: 6.0 Contact Time: 200 min Temp.: 25°C	438.8 mg/g	[45]
Mg-Al-CO_3	NP: <3 mg/L pH: 7.0–9.0 Contact Time: 10 min Temp.: Ambient	88–93%	[46]
WO_3/TNAs (Tungsten trioxide/Nanotube arrays)	NP: 2mg/L pH: 6.5–7.5 Contact Time: 120 min. Temp.: Ambient	> 97%	[47]
Pectin-Fe_3O_4	NPEO: 20 mg/L pH:7 Contact Time: 60 min.	62%	[48]
BT-Fe_3O_4	NPEO: 10 mg/L pH: 7.0 Contact Time: 60 min Temp.: Ambient	73.3%	This Study

Table 2. The isotherm models and their constants

Langmuir Model		**Freundlich Model**	
$\frac{1}{q_e}=\frac{1}{bq_mC_e}+\frac{1}{q_m}$		$\ln q_e=\ln K_f+\frac{1}{n}\ln C_e$	
Q (mg/g)	0.817	K_f (mg/g)(L/mg$^{1/n}$)	1.01
b (L/mg)	6.6375	n	2.28
R_L	0.0037	R^2	0.9739
R^2	0.9114		
Tempkin Model		Harkins-Jura Model	
$q_e=\frac{R.T}{b_T}.\ln\left(A_T.C_e\right)$		$\frac{1}{q_e^2}=\left(\frac{B}{A}\right)-\left(\frac{1}{A}\right)\log C_e$	
B_1	2.542	A	2.9472
K_T (L/g)	1.00	B	1.7020
R^2	0.7311	R_2	0.9572

q_e: amount adsorbed, b: Langmuir constant, C_e: equilibrium concentration q_m: monolayer adsorption capacity, K_f and n: Freundlich constants, R: constant, T: temperature, b_T and A_T: Tempkin isotherm constant, A and B: Harkins-Jura constants.

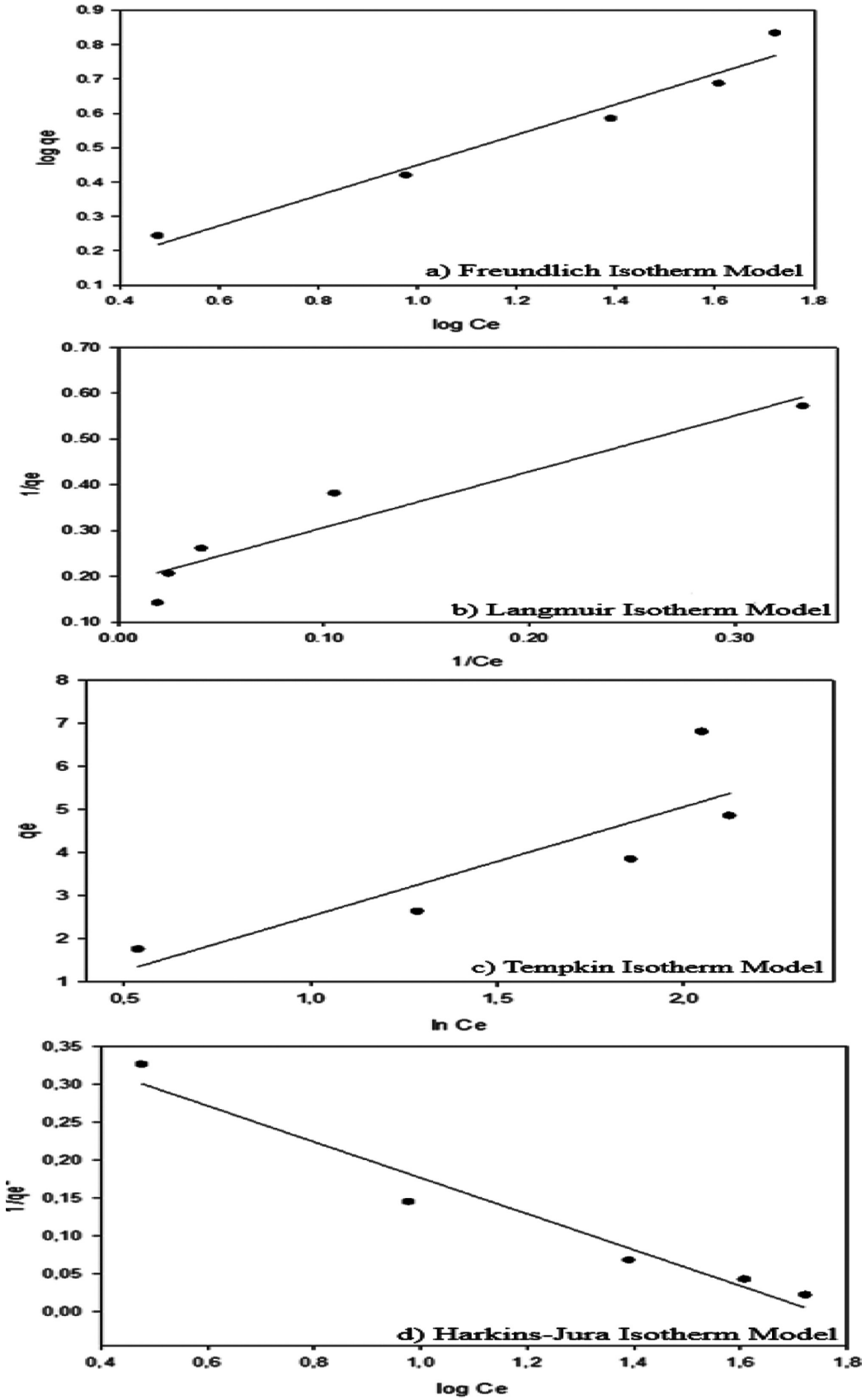

Figure 7. The isotherm modeling results of NPEO adsorption by BT-Fe_3O_4.

Sigma J Eng Nat Sci, Vol. 40, No. 1, pp. 132-143, March, 2022

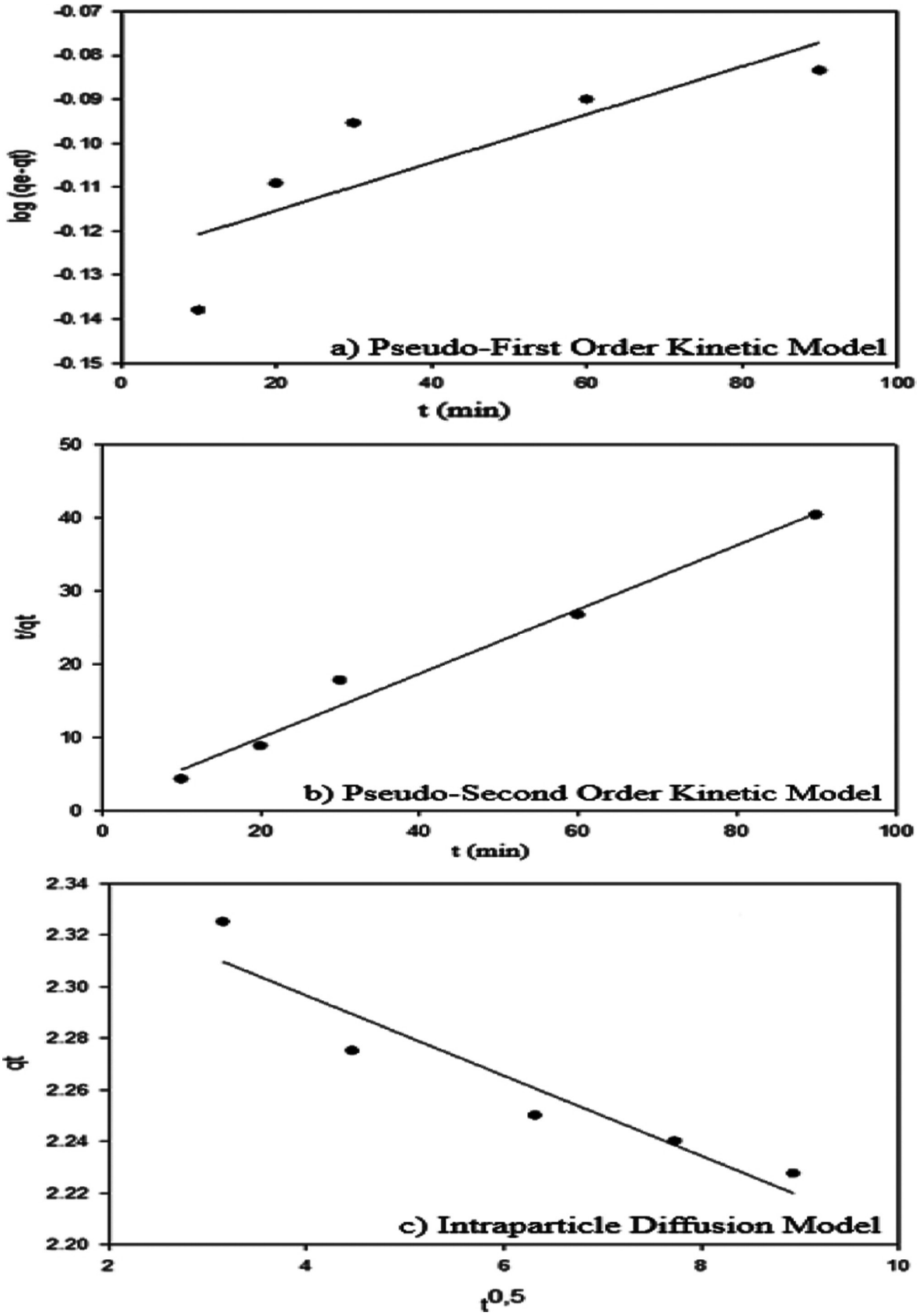

Figure 8. The kinetic modeling results of NPEO adsorption by BT-Fe_3O_4.

Table 3. The kinetic models and their constants

Pseudo-First Order Kinetic Model			Pseudo-Second Order Kinetic Model			Intraparticle Diffusion Model		
k_1 (l/min)	q_e (mg/g)	R^2	k_2 (l/min)	q_e (mg/g)	R^2	k_p (g.dk$^{0.5}$)	C (mg/g)	R^2
0.01	3.052	0.6818	18.66	2.279	0.9817	0.015	2.358	0.897
$\log(q_e - q_t) = \log q_e - \frac{k_1}{2.303} * t$			$\frac{1}{q_t} = \left[\frac{1}{k_2 * q_e^2}\right] + \frac{1}{q_e} * t$			$q_e = k_p t^{0.5} + C$		

k_1, k_2, and k_p: constant, C: boundary layer thickness.

Table 4. ANOVA analysis

		SS	df	MS	F	Sig.
pH	Between Groups	905.589	1	905.589	1014.188	.000
	Within Groups	16.073	18	.893		
	Total	921.661	19			
Nano-dose	Between Groups	1035.361	1	1035.361	372729.78	.000
	Within Groups	.050	18	.003		
	Total	1035.411	19			
Concentration	Between Groups	1106.789	1	1106.789	1.981	.176
	Within Groups	10058.491	18	558.805		
	Total	11165.281	19			

the adsorption process, kinetic experiments were carried out at 25°C with a nano-dose of 1 g/L and 10 mg/L NPEO concentration. The adsorption capacities were determined for the adsorption process of 10-90 min. The kinetic parameters and correlation coefficients (R^2) were summarized in Table 3 and Fig. 8 (a, b, and c).

STATISTICAL ANALYSIS

The empirical results obtained to explain the statistical significance of the proposed adsorption processes were analyzed using ANOVA (Table 4). ANOVA results are directly related to high F-value and low p-value [50]. F-values of the model as 1014.188 and 372729.78 implies the model is significant for pH and BT-Fe_3O_4 nano-dose, respectively. The probability that such a large F-value will occur due to noise is only 0.01%. P values smaller than 0.0500 showed that the model terms are meaningful. In this instance, pH and BT-Fe_3O_4 nano-dose are statistically important parameters. Values larger than 0.1000 showed the models are meaningless and the NPEO concentration is a meaningless parameter.

CONCLUSION

Black tea leaves and Fe_3O_4 particles were exposed to a green synthesize by chemical co-precipitation method to obtain BT-Fe_3O_4 nanoparticles, and these BT-Fe_3O_4 particles were applied as an efficient adsorbent for the removal of NPEO from a solution. It showed that the kinetic and isotherm models in NPEO removal fit the so-called second-order kinetic and Freundlich models. These models indicated that the process can occur by chemisorption and occur as a multilayer process. The ideal conditions in this paper were defined as pH 7.0, the contact time of 60 min, NPEO concentration of 10 mg/L, and adsorbent dose of 1.0 g/L. Moreover, the extract of black tea leaves was an efficient candidate for the green synthesis of magnetite nanoparticles. The results of this study showed that BT-Fe_3O_4 particles eco-friendly, cheap-cost particles for the treatment of NPEO from water and wastewater.

AUTHORSHIP CONTRIBUTIONS

Authors equally contributed to this work.

DATA AVAILABILITY STATEMENT

The authors confirm that the data that supports the findings of this study are available within the article. Raw data that support the finding of this study are available from the corresponding author, upon reasonable request.

CONFLICT OF INTEREST

The author declared no potential conflicts of interest with respect to the research, authorship, and/or publication of this article.

ETHICS

There are no ethical issues with the publication of this manuscript.

REFERENCES

[1] Vargas-Berrones K, Bernal-Jácome L, de León-Martínez LD, Flores-Ramírez, R. Emerging pollutants (EPs) in Latin América: A critical review of under-studied EPs, case of study-nonylphenol. Sci Total Environ 2020;726:138493. [CrossRef]

[2] Priac A, Morin-Crini N, Druart C, Gavoille S, Bradu C, Lagarrigue C, et al. Alkyl phenol and alkyl phenol polyethoxylates in water and wastewater: A review of options for their elimination. Arab J Chem 2017;10(Suppl 2):S3749–S3773. [CrossRef]

[3] Qiu L, Dong Z, Sun H, Li H, Chang CC. Emerging pollutants–part i: occurrence, fate and transport. Water Environ Res 2016;88:1855–1875. [CrossRef]

[4] da Silva APA, de Oliveira CDL, Quirino AMS, da Silva FDM, de Aquino Saraiva R et al. Endocrine disruptors in aquatic environment: effects and consequences on the biodiversity of fish and amphibian species. Aqua Sci Technol 2018;6:35–51. [CrossRef]

[5] Shao B, Hu J, Yang M, An W, Tao S. Nonylphenol and nonylphenol ethoxylates in river water, drinking water, and fish tissues in the area of Chongqing, China. Arch Environ Contam Toxicol 2005;48:467–473. [CrossRef]

[6] Brix R, Postigo C, González S, Villagrasa M, Navarro A, Kuster M, et al. Analysis and occurrence of alkylphenolic compounds and estrogens in a European river basin and an evaluation of their importance as priority pollutants. Anal Bioanal Chem 2010;396:1301–1309. [CrossRef]

[7] Hussain I, Li M, Zhang Y, Li Y, Huang S, Du X, et al. Insights into the mechanism of persulfate activation with nZVI/BC nanocomposite for the degradation of nonylphenol. Chem Eng J 2017;311:163–172. [CrossRef]

[8] Kinney CA, Furlong ET, Zaugg SD, Burkhardt MR, Werner SL, Cahill JD, et al. Survey of organic wastewater contaminants in biosolids destined for land application. Enviro Sci Technol 2006;40:7207–7215. [CrossRef]

[9] Soares A, Guieysse B, Jefferson B, Cartmell E, Lester JN. Nonylphenol in the environment: a critical review on occurrence, fate, toxicity and treatment in wastewaters. Environ Int 2008;34:1033–1049. [CrossRef]

[10] Jobling S, Williams R, Johnson A, Taylor A, Gross-Sorokin M, Nolan M, et al. Predicted exposures to steroid estrogens in UK rivers correlate with widespread sexual disruption in wild fish populations. Environ Health Perspect 2006;114:32–39. [CrossRef]

[11] Laws SC, Carey SA, Ferrell JM, Bodman GJ, Cooper RL. Estrogenic activity of octylphenol, nonylphenol, bisphenol and methoxychlor in rats. Toxicol Sci 2000;54:154–167. [CrossRef]

[12] Arlos MJ, Parker WJ, Bicudo JR, Law P, Hicks KA, Fuzzen MLM, et al. Modeling the exposure of wild fish to endocrine active chemicals: Potential linkages of total estrogenicity to field-observed intersex. Water Res 2018;139:187–197. [CrossRef]

[13] Vilela CLS, Bassin JP, Peixoto RS. Water contamination by endocrine disruptors: Impacts, microbiological aspects and trends for environmental protection. Environ Pollu 2018;235:546–559. [CrossRef]

[14] Gao D, Li Z, Guan J, Liang H. Seasonal variations in the concentration and removal of nonylphenol ethoxylates from the wastewater of a sewage treatment plant. J Environ Sci 2017;54:217–223. [CrossRef]

[15] Araujo FG, Bauerfeldt GF, Cid YP. Nonylphenol: properties, legislation, toxicity and determination. Anais da Academia Brasileira de Ciências 2018;90:1903–1918. [CrossRef]

[16] Sepehri A, Sarrafzadeh MH. Effect of nitrifiers community on fouling mitigation and nitrification efficiency in a membrane bioreactor. Chemical Engineering and Processing-Process Intensification 2018;128:10–18. [CrossRef]

[17] Rani M, Shanker U. Sun-light driven rapid photocatalytic degradation of methylene blue by poly (methyl methacrylate)/metal oxide nanocomposites. Colloid Surf A: Physicochem Eng Asp 2018;559:136–147. [CrossRef]

[18] Rani M, Shanker U. Metal oxide-chitosan based nanocomposites for efficient degradation of carcinogenic PAHs. J Environ Chem Eng 2020;8:103810. [CrossRef]

[19] Rani M, Shanker U. Efficient photocatalytic degradation of Bisphenol A by metal ferrites nanoparticles under sunlight. Environ Technol Innov 2020;19:100792. [CrossRef]

[20] Khalaj M, Kamali M, Costa MEV, Capela I. Green synthesis of nanomaterials-a scientometric assessment. Journal of Cleaner Production 2020;267:122036. [CrossRef]

[21] Zambre A, Upendran A, Shukla R, Chanda N, Katti KK, Cutler C, et al. Green nanotechnology-a sustainable approach in the nanorevolution. In: Luque R, Varma RS, editors. Sustainable Preparation of Metal Nanoparticles. 1st ed. London: Royal Society

of Chemistry; 2012:144–156. [CrossRef]
[22] Hwang YH, Kim DG, Shin HS. Effects of synthesis conditions on the characteristics and reactivity of nano scale zero valent iron. Appl Catal B 2011;105:144–150. [CrossRef]
[23] Kamali M, Persson KM, Costa ME, Capela I. Sustainability criteria for assessing nanotechnology applicability in industrial wastewater treatment: current status and future outlook. Environ Int 2019;125:261–276. [CrossRef]
[24] Rafique M, Sadaf I, Rafique MS, Tahir MB. A review on green synthesis of silver nanoparticles and their applications. Artif Cells Nanomed Biotechnol 2017;45:1272–1291. [CrossRef]
[25] Singh J, Dutta T, Kim KH, Rawat M, Samddar P, Kumar P. Green synthesis of metals and their oxide nanoparticles: applications for environmental remediation. J Nanobiotechnol 2018;16:84. [CrossRef]
[26] Mukunthan KS, Balaji S. Silver nanoparticles shoot up from the root of Daucus carrota (L.). Int J Green Nanotechnol 2012;4:54–61. [CrossRef]
[27] Mohanpuria P, Rana NK, Yadav SK. Biosynthesis of nanoparticles: technological concepts and future applications. J Nanopart Res 2008;10:507–517. [CrossRef]
[28] Krishnaraj C, Muthukumaran P, Ramachandran R, Balakumaran MD, Kalaichelvan PT. Acalypha indica linn: biogenic synthesis of silver and gold nanoparticles and their cytotoxic effects against MDA-MB-231, human breast cancer cells. Biotechnol Rep 2014;4:42–49. [CrossRef]
[29] Cheera P, Karlapudi S, Sellola G, Ponneri V. A facile green synthesis of spherical Fe3O4 magnetic nanoparticles and their effect on degradation of methylene blue in aqueous solution. J Mol Liq 2016;221:993–998. [CrossRef]
[30] Huang H, Li H, Wang AJ, Zhong SX, Fang KM, Feng JJ. Green synthesis of peptide-templated fluorescent copper nanoclusters for temperature sensing and cellular imaging. Analyst 2014;139:6536–6541. [CrossRef]
[31] Shah RK, Boruah F, Parween N. Synthesis and characterization of ZnO nanoparticles using leaf extract of *Camellia sinesis* and evaluation of their antimicrobial efficacy. Int J Curr Microbiol Appl Sci 2015;4:444–450.
[32] Huang L, Weng X, Chen Z, Megharaj M, Naidu R. Green synthesis of iron nanoparticles by various tea extracts: comparative study of the reactivity. Spectrochim Acta A Mol Biomol Spectrosc 2014;130:295–301. [CrossRef]
[33] Petcharoen K, Sirivat A. Synthesis and characterization of magnetite nanoparticles via the chemical co-precipitation method. Mater Sci Eng B 2012;177:421–427. [CrossRef]
[34] Nanditha A, Manokaran J, Balasubramanian N. Fabrication of Lys-PVA-Fe3O4 modified electrode for the electrochemical determination of uric acid. Research Journal of Chemistry and Environment 2014;18:54–61. [CrossRef]
[35] Wan S, Ma Z, Xue Y. Sorption of lead (II), cadmium (II), and copper (II) ions from aqueous solutions using tea waste. Ind Eng Chem Res 2014;53:3629–3635. [CrossRef]
[36] Karatapanis AE, Fiamegos Y, Stalikas CD. Silica-modified magnetic nanoparticles functionalized with cetylpyridinium bromide for the preconcentration of metals after complexation with 8-hydroxyquinoline. Talanta 2011;84:834–839. [CrossRef]
[37] Babaei AA, Mesdaghiniai AR, Haghighi NJ, Nabizadeh R, Mahvi AH. Modeling of nonylphenol degradation by photo-nanocatalytic process via multivariate approach. J Hazard Mater 2011;185:1273–1279. [CrossRef]
[38] Pan J, Li L, Hang H, Ou H, Zhang L, Yan Y, et al. Study on the nonylphenol removal from aqueous solution using magnetic molecularly imprinted polymers based on fly-ash-cenospheres. Chem Eng J 2013;223:824–832. [CrossRef]
[39] Salimi J, Kakavandi B, Babaei AA, Takdastan A, Alavi N et al. Modeling and optimization of nonylphenol removal from contaminated water media using a magnetic recoverable composite by artificial neural networks. Water Sci Technol 2017;75:1761–1775. [CrossRef]
[40] Shu HY, Chang MC, Chen CC, Chen PE. Using resin supported nano zero-valent iron particles for decoloration of acid blue 133 azo dye solution. J Hazard Mater 2010;184:499–505. [CrossRef]
[41] Soltani RDC, Khorramabadi GS, Khataee AR, Jorfi S. Silica nanopowders/alginate composite for adsorption of lead (II) ions in aqueous solutions. J Taiwan Inst Chem Eng 2014;45:973–980. [CrossRef]
[42] Ahmadi M, Vahabzadeh F, Bonakdarpour B, Mofarrah E, Mehranian M. Application of the central composite design and response surface methodology to the advanced treatment of olive oil processing wastewater using Fenton's peroxidation. J Hazard Mater 2005;123:187–195. [CrossRef]
[43] Khatibikamal V, Panahi HA, Torabian A, Baghdadi M. Optimized poly (amidoamine) coated magnetic nanoparticles as adsorbent for the removal of nonylphenol from water. Microchem J 2019;145:508–516. [CrossRef]
[44] Li X, Chen S, Li L, Quan X, Zhao H. Electrochemically enhanced adsorption of nonylphenol on carbon nanotubes: Kinetics and isotherms study. J Colloid Interface Sci 2014;415:159–164. [CrossRef]
[45] Pan J, Li L, Hang H, Ou H, Zhang L, Yan Y, et al. Study on the nonylphenol removal from aqueous

Sigma J Eng Nat Sci, Vol. 40, No. 1, pp. 132-143, March, 2022

solution using magnetic molecularly imprinted polymers based on fly-ash-cenospheres. Chem Eng J 2013;223:824–832. [CrossRef]

[46] Kostura B, Škuta R, Plachá D, Kukutschová J, Matýsek D. Mg–Al–CO3 hydrotalcite removal of persistent organic disruptor—Nonylphenol from aqueous solutions. Appl Clay Sci 2015;114:234–238.

[47] Xin Y, Gao M, Wang Y, Ma D. Photoelectrocatalytic degradation of 4-nonylphenol in water with WO3/TiO2 nanotube array photoelectrodes. Chem Eng J 2014;242:162–169. [CrossRef]

[48] Uysal, Y, Belibağlı, P. Removal of nonylphenol ethoxylates from water by using pectin coated nano magnetite composite (Pectin-Fe3O4). Pamukkale Univ J Eng Sci 2019;25:929–937. [CrossRef]

[49] Febrianto J, Kosasih AN, Sunarso J, Ju YH, Indraswati N. Equilibrium and kinetic studies in adsorption of heavy metals using biosorbent: a summary of recent studies. J Hazard Mater 2009;162:616–645. [CrossRef]

[50] Srivastava V, Sharma YC, Sillanpää M. Response surface methodological approach for the optimization of adsorption process in the removal of Cr (VI) ions by Cu2(OH)2CO3 nanoparticles. Appl Surf Sci 2015;326:257–270. [CrossRef]